10/8/19/91 wb (1)

8-7-91

SANDIA REPORT

SAND90—0626 • UC—721
Unlimited Release
Printed July 1991

Summary of WIPP Room B Heater Test Brine and Backfill Material Data

J. L. Krumhansl, C. L. Stein, G. D. Jarrell, K. M. Kimball

Prepared by
Sandia National Laboratories
Albuquerque, New Mexico 87185 and Livermore, California 94550
for the United States Department of Energy
under Contract DE-AC04-76DP00789

Issued by Sandia National Laboratories, operated for the United States Department of Energy by Sandia Corporation.

Available to DOE and DOE contractors from
Office of Scientific and Technical Information
PO Box 62
Oak Ridge, TN 37831

Prices available from (615) 576-8401, FTS 626-8401

Available to the public from
National Technical Information Service
US Department of Commerce
5285 Port Royal Rd
Springfield, VA 22161

NTIS price codes
Printed copy: A03
Microfiche copy: A01

SAND90-0626
Unlimited Release
Printed July 1991

SAND--90-0626

DE91 016871

Summary of WIPP Room B Heater Test Brine and Backfill Material Data

J. L. Krumhansl, C. L. Stein, G. D. Jarrell, and K. M. Kimball
Geochemistry Division, 6233
Sandia National Laboratories
Albuquerque, NM 87185

Abstract

Simulated DHLW (Defense High Level Waste) package performance tests were carried out at the WIPP (Waste Isolation Pilot Plant) by emplacing a number of waste canisters containing electrical heaters into the floor of the mine. Peak temperatures were about 130°C, and the tests ran for three years. During this time, an unanticipated large amount of water was collected from heater hole B042. A study was, therefore, undertaken to determine if this fluid was derived from normal weep brines. This was accomplished by comparing the amount of salt deposited by the dried weep brines with the volume of condensed steam collected during the test. In sampling this condensate, it was noted that the fluid was strongly acid (pH 0.7). High temperature hydrolysis of the magnesium from the brine was found to be the cause of this acid condition, so the effect is of no relevance to a low-level waste repository.

Documenting the post-test condition of the various backfills was the other objective of this report. In spite of being exposed to acidic vapors, the bentonite-sand backfill retained its mineralogic integrity. However, the bentonite-sand backfill compacted between the canister and the wall only achieved a density that was about three quarters that of a pore-free material. The bentonite backfill also showed evidence of hair-line cracks through which steam had left the vicinity of the canister. In contrast, compacted crushed salt backfill exhibited no evidence of through-going cracks and was compacted to better than 99% of that of pure nonporous sodium chloride. Thus, the seal provided by a crushed salt backfill appears to be superior to that provided by bentonite.

This Page Intentionally Left Blank

Contents

Tables

This Page Intentionally Left Blank

INTRODUCTION

The Waste Package Performance Technology Experiments for Simulated DHLW (Defense High Level Waste) are a series of in situ experiments to evaluate the performance of barrier materials interposed between waste and the host rock of a repository (Molecke, 1984). The tests were carried out at a depth of about 2150 feet in salt beds of the lower Salado Formation at the WIPP (Waste Isolation Pilot Plant), near Carlsbad, New Mexico. Each test consisted of a full-sized waste canister fabricated from a programmatically relevant alloy (Table 1).

Table 1
Heater Test Specifications

Heater	B047	B048	B042	B045
Canister Material	TiCode	TiCode	Steel	Steel
Backfill	Bent.+Sand	Bent.+Sand	None	Crushed Salt
Hole Diameter#	36"	36"	36"	36"
Canister Diameter	24"	24"	24"	24"
Brine Injected ##	100 ml	100 ml	None	100 ml

Canisters were emplaced vertically into holes in the mine floor such that the top of the can was about 88 inches below the mine floor. Each heater was sealed at the top with an air-tight cap. Heat was supplied internally by Calrod electric heating elements. The maximum hole wall temperature for most of the test was about 130°C. A variety of conditions existed in the annular spaces between the canisters and hole walls. In some cases, such as with B042, the hole was simply left empty after the heater was inserted. In other experiments, the remaining space was filled with crushed rock salt (B045) or 70% wt. bentonite clay mixed with 30% wt. silica sand (B047 and B048). In every case the salt deformed plastically during the tests so that the free space in the hole was eliminated. In the process, this either compacted the backfill or, when no intervening material existed, brought rock salt into direct contact with the heater.

This report summarizes a variety of observations made relative to the influence of brine during these tests. Initially, the question of how much brine actually entered heater hole B042 is considered in some detail. This is of importance because, unlike heater hole B048 that received about 100 l of artificially introduced brine A (Molecke, M.A., 1983), the flow into B042 was all natural fluid derived from the formation. The next matter addressed is the ability of boiling brine to create strongly acidic environments around the experiments. Finally, the relative performance of crushed salt and bentonite backfills are evaluated.

HEATER B042 SITE STUDIES

Assessing the amount of natural weep brine likely to migrate toward a heater (or to a waste canister) was an important objective of these tests (Nowak, 1985). Hence, the space between the canister and hole wall was continuously purged with dry nitrogen, and the scavenged moisture was recovered by passing the gas over a molecular sieve specific to water (Nowak and McTigue, 1987). The general pattern of brine influx found involved a high initial delivery rate that fell with time. In the first 600 days a total of 35 l of brine were collected. Because this amount of brine has significant technical implications, an independent check on this figure was sought. This was performed by measuring the amount of salt deposited from the dried weep brines, and then using that value to estimate the total brine influx into the heater hole.

The condensate was also found to be so acidic that it readily corroded the stainless steel fittings in the collection system. A combined theoretical and laboratory approach is taken to demonstrate that this condition was a natural consequence of drying a typical weep brine at temperatures above about 100°C. Finally, the mild steel corrosion products forming on the canister surface are documented.

Estimate of Brine Influx based on Weep Salt Deposition

At the termination of the experiment, the heater and adjacent salt were recovered using a 37 inch core barrel. After removing the core from the hole, the exterior surface of the heated canister was exposed by splitting off the six inch thick skin of rock salt comprising the outer part of the core. At this point, it became apparent that during the test the rock salt had flowed inward eliminating the space that originally existed between the canister and the hole wall. Caught between the canister and the rock salt was a porous irregular layer of discolored salts (Table 2). In part, this layer was comprised of salts left behind by evaporating weep brines. Because of the hole closure, however, it was impossible to assess whether these salts were initially deposited on the canister surface or the hole wall. This layer was also contaminated with crushed salt (used to seal the top of the hole), rust (from the canister), and in the hole bottom, silica sand. In general, the layer was thinnest and appeared to be least contaminated over the midsection of the canister. Table 2 summarizes the apparent thicknesses of these accumulations.

At first glance, it might seem that this data could be used to estimate the brine influx. However, three factors preclude such an application: (1) in both the top and bottom of the hole, crushed rock salt from the formation collected and contributed to the mass of material in the annulus, (2) the dried weep salts form a porous mass that is distributed in an irregular, patchy manner, and (3) much of the material accumulated over the midsection of the heater is rust rather than salts deposited from dried weep fluids.

Table 2
Thickness of Salts Deposited on Heater B042

Distance From Bottom (inches)	Thickness (inches)	Distance From Bottom (inches)	Thickness (inches)
0 *	2	60	0.20
6 *	2	72	0.20
9 *	1.5	89	0.20
12 *	0.75	90	0.38
18	0.44	93	0.38
24	0.31	96 *	0.56
36	0.25	102 *	0.75
48	0.20	110 *	1.06

*Powdered salt or sand adds to the amount of material accumulated.

Because of its heteogeneous nature, an analytic procedure was required to quantitatively evaluate the amount of weep salt incorporated into the layer between the canister surface and the rock salt. Several large sections of overcored salt came off the canister intact, covering about 84 percent of the total canister surface area. A portion of the dried weep salts remained on the inner surface of the overcore, while the rest remained firmly attached to the heater. The material on the heater was sampled by scraping off all the salts (along with some rust from the corroded heater) in a 1 foot wide strip over the length of the heater. The weep salts were also removed from the inner surface of the overcore, though this required a somewhat different technique. Pieces of overcore were first divided into one foot sections and the area measured (Fig.1). The inner surface was then chipped off with a pneumatic chisel. These chips were then collected and weighed. Next, the chips were leached with deionized water to determine how much rust was incorporated into the samples. The resulting solution was also analyzed to determine the proportions of rock salt and weep salts in the samples. Taken together, this information was then used to estimate the amount of brine that had flowed into the hole (Appendix A).

Depending on the assumptions used, these calculations implied that anywhere between 20 and 23 l of water might have entered the hole. In comparing these numbers with the field test data, it is important to realize that once the hole wall was above the boiling point of brine, additional salts could not be deposited by brine drying on the hole wall. Consequently, weep salt accumulation at the interface would cease, even though boiling behind the interface continued to contribute steam to the hole (which then could be collected). Taking a Time - Wall Temperature profile at the heater midplane (Fig. 2B - taken from Nowak and McTigue, 1987), it was estimated that this occurred sometime between 250 and 400 days into the test. Longer times are more likely because in order for salt accumulation to effectively stop more than just the midsection of the hole, it would have to reach the brine boiling point. Nowak and McTigue (1987) found that the cumulative brine influx at 250 days was about 15.5 l, and at 400 days about 26.5 l (Fig 2A). In short, there is remarkably good agreement between the fluid volumes collected during the field test, and the influx predicted based on the residual salts. It also follows that the fluid collected during the test can be ascribed to normal weep fluids, and is not a manifestation of some extraneous unanticipated moisture source.

Source of Acid Condensate

The other feature of this particular heater experiment was the highly acidic nature of the condensate. Values as low as pH 0.7 were routinely measured in the field. Further, the dark green color imparted by the dissolved nickel (from instrumentation of test hardware), suggested that some of the hydrogen ion initially in solution had also been consumed through corrosion of Inconel fittings in the collection line prior to making the pH measurement. The origin of the acid in the condensate has been recognized for some time (Krumhansl, 1986, Sandia Internal Memo to M.A. Molecke) as the hydrolysis of the magnesium salts deposited from the weep fluids. This was verified experimentally by taking WIPP salts, placing them at the bottom of a closed quartz tube and then placing the lower half of the tube in a furnace at various temperatures. The condensate forming in the cool end of the tube was collected and the pH value measured (Fig. 3). At temperatures below 350°C, there was no odor of sulfur therefore, HCl was the principal acid given off. Above this temperature, a distinctly sulfurous smell was detected so that under these conditions, sulfuric acid can apparently be evolved by the hydrolysis of magnesium sulfate.

The process of acid generation was investigated further by boiling an idealized weep fluid (26.82 g NaCl, 23.75 g $MgCl_2.6H_2O$, 4.87 g KCl, 3.27g Na_2SO_4, 100 g H_2O) to dryness. The first condensate derived from boiling fluid at 106°C had a pH of 3.5. As boiling progressed, the condensate pH gradually climbed to around 4.7. Finally, as the crystal mush congealed and the last water was lost, the condensate pH plummeted to around 1.2. The experiment was extended further by slowly dripping water on the salt cake and collecting the condensate. The rate of water addition was adjusted so that the salt cake remained just moist enough that a trace of boiling brine resided in the pores in the bottom of the salt cake. The temperature of the brine saturated salt cake was variously measured as being between 115 and 160°C.

In this manner 3.5 ls of fluid was passed over the salts deposited in the bottom of the flask. The pH of this condensate varied between 1.9 and 2.0. The phases detected in the dried salts from the flask include halite Hace, Carnallite ($KMgCl_3.6H_2O$), KCl (sylvite), and possibly traces of $Mg(OH)_2$, $Mg_2(OH)_3Cl$, and bischofite ($MgSO_4.6H_2O$). Halite, carnallite and traces of sylvite, kieserite, and bischofite were also detected in x-ray diffraction patterns obtained from salts deposited on the heater (Table 3).

Table 3
Mineralogy of B042 Heater Scale
(Distance are downward from the top of the heater)

JS 57 From 0 to 1 foot down - halite.

JS 58 From 1 to 2 feet down - mostly halite and traces of bischofite and sylvite.

JS 59 From 2 to 3 down - mostly halite, a few good carnallite x-ray diffraction peaks (a few important ones missing between 24 and 26.5°). Possibly traces of kieserite, bischofite and sylvite.

JS 60 From 3 to 4 feet down - mostly halite but the carnallite x-ray diffraction peaks are well represented in this sample; possibly a trace of bischofite also.

JS 61 From 4 to 5 feet down - halite, carnallite and sylvite.

JS 62 From 5 to 6 feet down - some small clear gemmy non-cubic crystals which proved to be pure carnallite. The bulk of the sample was halite with a lesser, but significant, amount of carnallite. May contain traces of bischofite as well.

JS 63 From 6 to 7 feet down - halite and probably a little carnallite.

JS 64 From 7 to 8 feet 4 inches down - halite and a definite, though minor, amount of carnallite. (This sample originated from the junction between the bottom of the weep salt accumulations and the top of the crushed salt filling the hole bottom)

JS 65 From 8 feet 4 inches to the heater bottom. Essentially pure halite.

JS 66 Hardpan heater scale taken from the dense salt - halite and possibly a little bischofite.

None of the pH values obtained experimentally, however, are as low as those obtained in the field. This discrepancy can be readily explained from theoretical arguments, based on a simplified model of the acid generation process:

$$KMgCl_3.6H_2O \text{ --------> } KCl + Mg(OH)_2 + 2HCl + 4H_2O \qquad (1)$$

The van't Hoff equation was employed to calculate the influence of temperature and steam pressure variations on the efficiency of the acid production mechanism illustrated by Equation (1), (Table 4). The enthalpy for carnallite at 25°C was taken from Naumov, et al.(1971) the free energy of carnallite at 25°C came from Harvie et al., (1984) and the remaining thermodynamic data were taken from Robie, et al (1978). Unfortunately, only qualitative agreement between calculations and experimental and field test data are possible (Fig. 3). This arises because of the poor quality of the thermochemical data available for carnallite, and because complex salts such as $Mg_2(OH)_2Cl_2.nH_2O$ may, in fact, form in preference to brucite ($Mg(OH)_2$) as stated above (1):

Table 4
Condensate pH Calculated for Reaction

T	P-Steam			
(°C)	1 atm	0.5 atm	0.1 atm	0.01 atm
100	6.4	5.5	3.4	0.4
115	5.2	4.3	2.2	-0.8
130	4.1	3.2	1.1	---
150	2.8	1.9	-0.2	---

These results illustrate three features of the physical chemistry of this reaction. One, condensate pH clearly decreases sharply as the source-term temperature rises. Thus, steam produced at the midplane is likely to be far more acidic than that produced at either end of a heater. Secondly, and of great importance since the heater cavity was constantly purged by dry nitrogen (to collect the water), is the fact that HCl production is much enhanced if the partial pressure of water vapor is kept low (Fig. 3). In fact, the lower right part of Table 3 illustrates a situation where virtually all the water present in a system is converted to hydrochloric acid. This is probably why the pH of condensate from the field experiments was so much lower than that of the laboratory studies, since the latter were all done at essentially one atmosphere of steam pressure. Finally, heat and dissolved magnesium are all that are required to make acid. Hence, the brine A that was introduced artificially to "overtest" the durability of certain canisters should have been as effective as producing acid as the natural weep brine.

Iron Corrosion Products

Canister corrosion products were found to be dominated by three phases, the minerals magnetite (Fe_3O_4), limonite (FeO(OH)), and akaganeite (β-FeO(OH,Cl)). The corrosion products also contained a high proportion of amorphous material (principally hydrous iron oxide). This follows from the observation that the peaks obtainable by x-ray diffraction were relatively weak reflections in proportion to the amount of material in the sample being x-rayed.

Examination of the rust with a scanning electron microscope equipped with an EDS unit for semiquantitative elemental analysis contributed further

to the catalogue of phases formed due to corrosion. In particular, a bladed material (Fig. 4) occurred repeatedly. The composition, however, is variable as illustrated by the contrasting results obtained when four similarly crystallized areas were analyzed (Table 5). This is obviously a salt of considerable complexity, with variable amounts of sodium, magnesium, sulfate, and chloride in addition to the hydrous iron oxides typical of rust. Other components such as Al and Si probably reflect a small amount of contamination from formation clays.

Table 5
Compositions (atom %) of phases such are illustrated in Fig. 4

	Sample 1	Sample 2	Sample 3	Sample 4
%Na	4.25	8.85	1.22	4.35
%Mg	5.59	25.23	5.44	7.54
%Al	0.31	0.00	1.57	0.54
%Si	0.63	0.29	4.85	1.35
%S	2.46	3.95	1.16	1.38
%Cl	5.57	6.82	1.16	1.85
%K	0.77	1.09	0.58	0.43
%Ca	0.17	0.14	0.13	0.09
%Fe	31.41	5.42	30.95	32.32
%Ti	0.02	0.00	0.00	0.05
%O*	48.83	48.20	52.95	50.10

* Oxygen by difference

OBSERVATIONS REGARDING BACKFILL PERFORMANCE

Once the extent of acid generation was realized, it was also recognized that a detailed mineralogic study of the heated bentonite would be a necessary part of the post-test backfill characterization process. Whereas the mineralogical stability of bentonite at these temperatures had previously been investigated (Krumhansl, 1984; Couture, 1985; Allen et al., 1984), none of these studies had anticipated the possibility of strongly acidic conditions. Even at modest temperatures, the author has found that in acidic aqueous systems bentonite reacts rapidly forming kaolinite, hematite, and amorphous silica. Further, the occurrence of kaolinite as an alteration product of the rocks surrounding acidic hot springs systems (i.e., Ellis and Mahon, 1977) shows such changes occur commonly in nature, as well as in laboratory experiments. If this happened in an actual repository, it could have a detrimental effect on a backfill's ability to sorb radionuclides or swell when wetted.

The backfill surrounding both B047 and B048 had areas of intense red discoloration along cracks where steam apparently escaped. Two samples of this material were selected (JS 92R and JS 95R), along with a sample of lighter colored bentonite-sand (JS 95W), that had been heated to a similar temperature. For comparison, a sample of unheated bentonite was also examined (JS 186). Samples were prepared for analysis by washing them free of soluble salts and then allowing a dilute suspension of the clay to dry on a glass slide. The possibility of gross mineralogic alteration was immediately ruled out when the x-ray diffraction pattern from the unheated bentonite (Lower Trace, Fig. 5) was found to be very similar to that of the

heated samples. In particular, note that there is no indication of a peak between 12.2 and 12.3° two theta, where the principal kaolinite peak would appear had this mineral formed to a significant degree.

In a search for more subtle changes, these four samples were also examined by transmission electron microscopy, but again no significant changes were apparent. Electron diffraction patterns (Fig. 7) complement the data obtained by x-ray diffraction because the former non-basal reflections are obtained (as would be the case with an unoriented clay mount), while the oriented clay mounts used for x-ray diffraction accentuate the (001) reflections. As with the x-ray diffraction, heated and unheated materials gave the same patterns (Fig. 7). The unheated clay (Fig 6A and 6B) appeared similar to the other samples (Fig. 6C - 6H), and there was not even a clear increase in the number of granular clumps high in iron (presumably the hematite responsible for the red coloration) in the heated materials. Finally, it was clear the compositions of the clays were not significantly altered by the process (Table 6).

Table 6
Thin Film X-ray Analysis of Clays

	Sample	%Si	%Mg	%Al	%K	%Ca	%Fe
				Heated Clay			
1	JS92R	63.7	4.3	25.5	0.8	1.4	4.2
2	JS92R	63.9	4.1	26.0	0.3	1.8	4.0
3	JS92R	62.4	4.2	26.0	0.4	2.2	4.8
4	JS95R	62.2	4.5	25.1	1.1	2.3	4.7
5	JS95R	63.3	6.4	24.5	0.5	1.5	3.9
6	JS95R	64.0	4.4	24.7	0.6	1.8	4.5
7	JS95W	62.1	3.4	27.9	0.6	2.5	3.6
8	JS95W	63.7	3.3	26.1	0.6	2.5	3.9
9	JS95W	63.4	3.5	26.1	0.6	1.6	4.8
				Unheated Clay			
10	JS186	62.9	4.1	25.8	1.0	1.6	4.7
11	JS186	63.0	3.4	26.8	1.1	1.4	4.2
12	JS186	63.7	3.0	27.2	1.1	1.9	3.2
13	JS186	63.3	3.1	26.1	0.7	1.8	5.1

* atom%

Error bars (in Weight Percent)

	Si%	Mg%	Al%	K%	Ca%	Fe%
1	2.0	0.2	0.8	0.1	0.1	0.2
2	2.0	0.2	0.8	0.0	0.1	0.2
3	1.9	0.2	0.8	0.0	0.1	0.2
4	1.9	0.2	0.8	0.1	0.1	0.2
5	2.0	0.3	0.8	0.0	0.1	0.2
6	2.0	0.2	0.8	0.0	0.1	0.2
7	1.9	0.2	0.9	0.0	0.1	0.2
8	2.0	0.2	0.9	0.1	0.1	0.2
9	2.0	0.2	0.9	0.0	0.1	0.2
10	1.9	0.2	0.8	0.1	0.1	0.2
11	1.9	0.2	0.9	0.1	0.1	0.2
12	2.0	0.2	0.9	0.1	0.1	0.1
13	2.0	0.2	0.9	0.1	0.1	0.2

The other post-test observation made on the backfill was a comparison of the influences of compaction on backfill performance. Density measurements made on bentonite samples obtained by coring between the hole wall and heater B047 ranged between 1.9 and 2.2 (g/cm^3). Since the theoretical grain density of this material is close to 2.7, it follows that this compacted material still had a considerable porosity. Porosity in the bentonite was not restricted to the small pores in the bulk material since the brick-red coloration noted along a number of hair-line cracks in the bentonite-sand backfill around B047 and B048 presumably reflect the passage of acid gases following brine injection. In contrast, the crushed salt backfill around the B045 heater was compacted to a density of 2.16; essentially that of pore-free sodium chloride. It also showed no sign that fluids having moved through the backfill, in spite of the 100 l of brine A were artificially injected at the start of the test. The tight seal formed by the crushed salt backfill limited corrosion to a small fraction of that found around similar mild steel canisters such as B042 where no backfill was used. (Parenthetically, unlike the mild steel canisters, the titanium-clad heaters showed no evidence of corrosion.)

Summary and Conclusions

The first part of this report addressed the influx of brine around heater B042. A method was devised, based on the accumulation of weep salts that verified brine influx measurements made by the on-line moisture collection system during the test. It follows that the brine entering this site was derived from normal weep fluids, and not from some anthropogenic source. In the course of this investigation, the chemical environment created by this evaporating brine was also examined. Of particular note was the acidic nature of the condensed steam collected from this hole.

At high temperatures the magnesium in the weep brines hydrolizes, resulting in acid formation. As the temperature falls, however, the equilibrium in reaction (1) shifts to the left. Consequently, this phenomenon will not occur in the WIPP if only low level (non heat producing) wastes are buried there. In examining materials from the heater surface, it

was found that carnallite was the principal bittern mineral deposited from the evaporating brine, and that a variety of materials were derived from the corroding mild steel canister (amorphous iron oxy-hydroxide, magnetite, limonite, akaganeite, an unnamed phase containing, in addition to iron and hydroxide, lesser amounts of sodium, magnesium, sulfate, and chloride). The extensive corrosion of the iron canisters stands in contrast to that observed on the titanium canisters, which at the test's conclusion appeared as fresh as when the test started.

The last half of this report documents the post-test condition of the bentonite-sand and crushed salt backfills emplaced around several of these canisters. At the conclusion of the test, no significant mineralogic alteration of the bentonite was observed. The red discoloration noted in some areas exposed to acidic vapors was traced to the formation of minute quantities of hematite. In comparing crushed salt and bentonite backfills, it appeared that the crushed salt did a better job of sealing around the canister. It compacted to essentially the density of pure salt, as compared to the density of compacted bentonite, that was only about 75% of that expected for pore-free material. Also, unlike the crushed salt, the bentonite backfill showed clear evidence that channels and cracks existed along which steam exited when brine was artificially injected. There is no evidence suggesting these features originated as a direct result of the brine injection. It is, therefore, concluded that they are an artifact of the compression occurring during hole closure. In terms of programmatic conclusions, it would appear that the rationale for including a bentonite backfill lies in its sorptive properties rather than its ability to provide a superior seal.

Bibliography

Allen, C.C., D.L. Lane, R.A. Palmer, and R.G. Johnson, 1984, Experimental studies of packing material stability, in G.L. McVay, Ed., Materials Research Society Symposium Proceedings, Vol. 26, North-Holland, 1984, p. 105-112.

Couture, R.A., 1985, Steam rapidly reduces the swelling capacity of bentonite, Nature, v. 318, pp. 50-52.

Ellis, A.J., and W.A.J. Mahon, 1977, Chemistry and Geothermal Systems, Academic Press, C.2 - Natural Hydrothermal Systems, pp .28-56.

Harvie, C.E., N. Moller, J.H. Weare, 1984, The prediction of mineral solubilities in natural waters: The $Na-K-Mg-Ca-H-Cl-SO_4-OH-HCO_3-CO_3-H_2O$ system to high ionic strengths at 25°C., Geochimica et Cosmochimica Acta, Vol. 48, pp. 723-751.

Krumhansl, J.L., 1984, Observations regarding the stability of bentonite backfill in a High-Level Waste (HLW) repository in rock salt, SAND83-1293, 86 pp.

Krumhansl, J.L., 1986 Sandia Internal Memo to M. A. Molecke: MIIT Heater Failure: Geochemical Analysis, April 1, 1986.

Krumhansl, J.L., C.L. Stein, K.M. Kimball, Mar. 1990, Intergranular Fluid Compositions from the Waste Isolation Pilot Plant (WIPP), Southeastern New Mexico, SAND90-0584.

Molecke, M.A., 1983, A Comparison of Brines Relevant to Nuclear Waste Experimentation, SAND83-0516.

Molecke, M.A., 1984, Test Plan: Waste Package Performance Technology Experiments for Simulated DHLW.

Naumov, G.B., B.N. Ryzhenko and I L. Khodakovsky, 1971, Handbook of Thermodynamic Data, Translated by G.J. Soleimani, U.S. Geological Survey, I. Barns and V. Speltz editors, 328 pp.

Nowak, E. J., 1985, Test Plan: Moisture release Experiment for Rooms A1 and B.

Nowak, E.J. and D.F. McTigue, 1987, Interim Results of Brine Transport Studies in the Waste Isolation Pilot Plant, SAND87-0880.

Robie, R.A., B.S. Hemingway and J.R. Fisher, 1978, Thermodynamic Properties of Minerals and Related Substances at 298.15 K and 1 Bar (10^5Pascals) Pressure and at Higher Temperatures, U.S. Geol. Survey Bull. 1452, 456 pp.

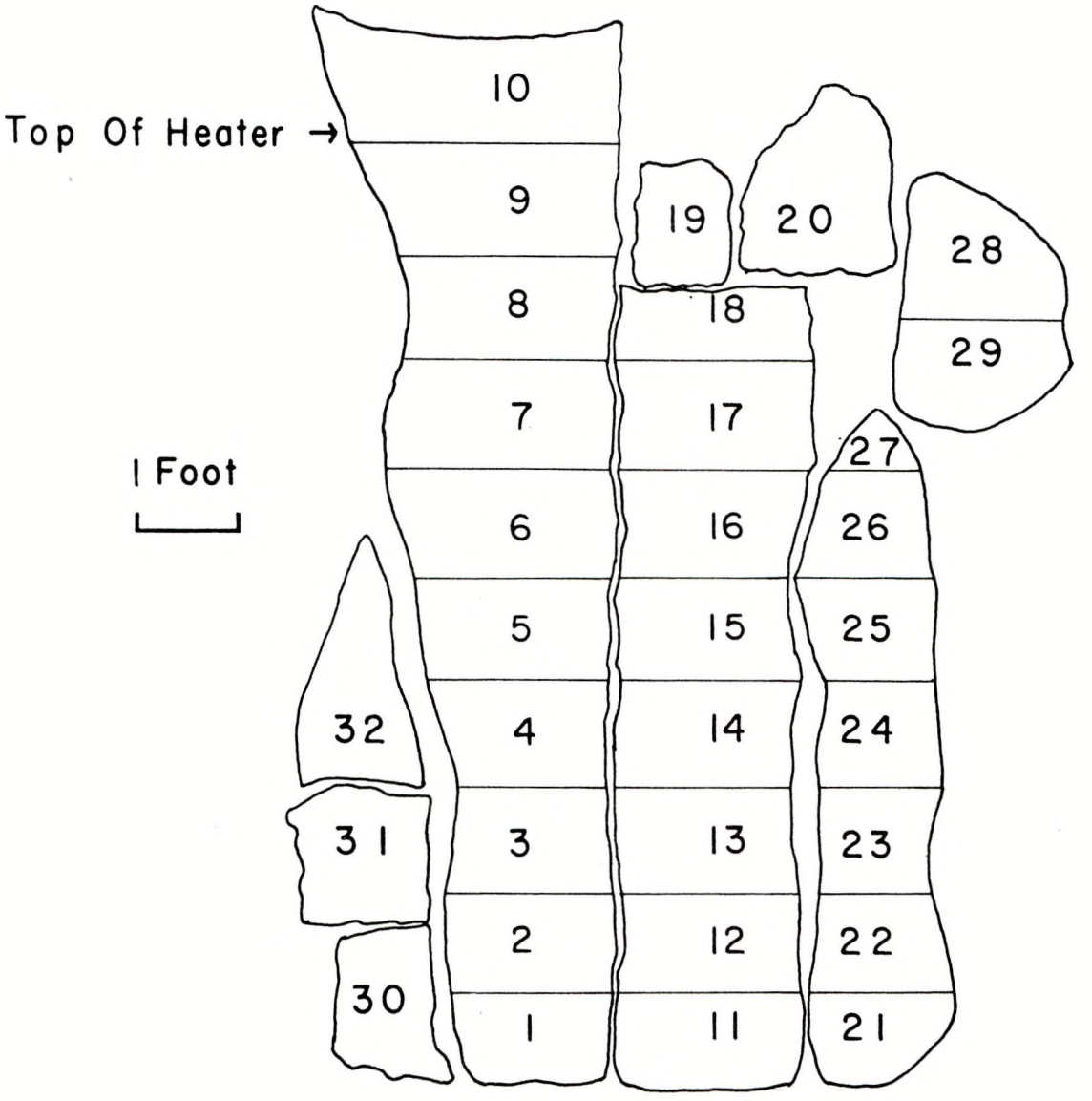
Top Of Heater →
1 Foot
10
9
8
7
6
5
4
3
2
1
19
20
18
17
16
15
14
13
12
11
28
29
27
26
25
24
23
22
21
32
31
30

Fig. 1

Fig. 2B

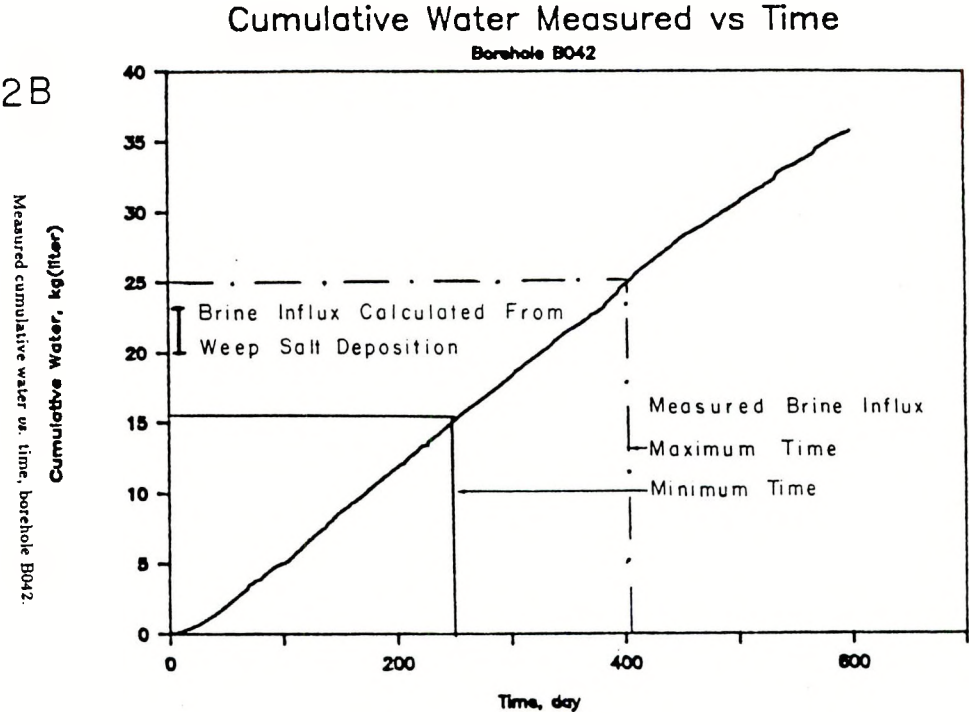

Measured cumulative water vs. time, borehole B042.

Fig. 2A

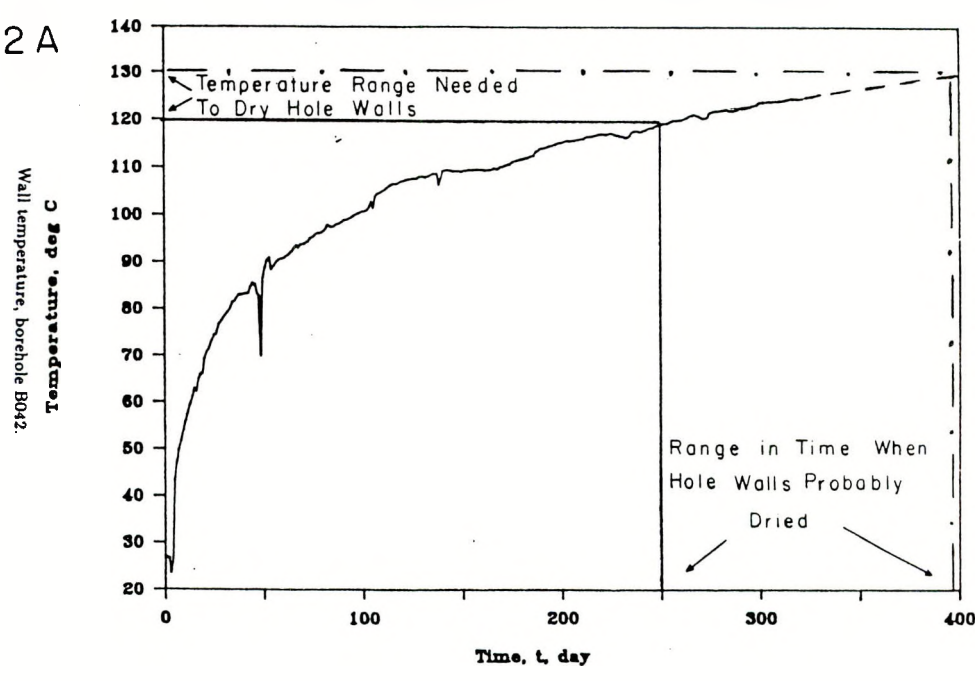

Wall temperature, borehole B042.

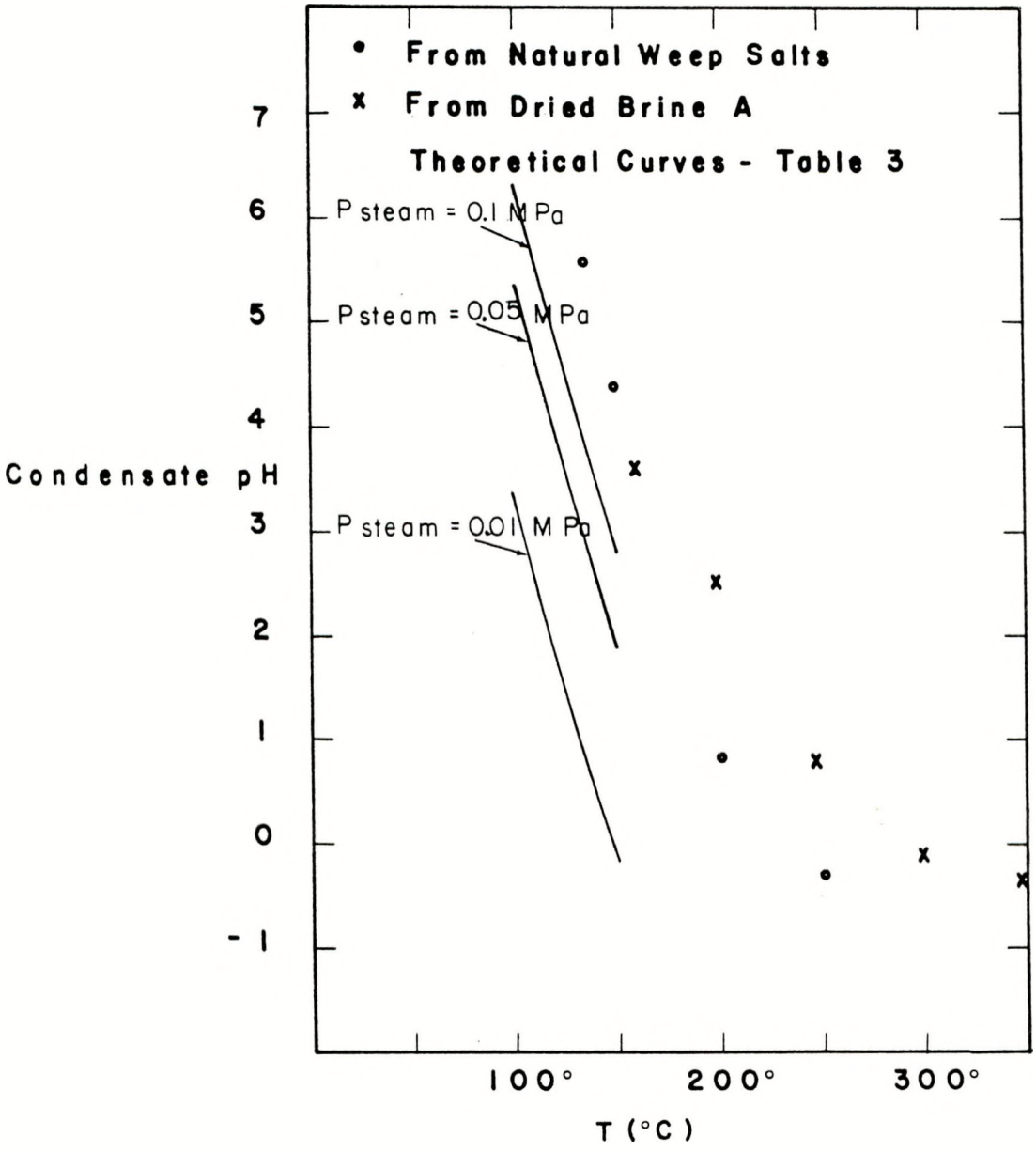
From Natural Weep Salts
From Dried Brine A
Theoretical Curves - Table 3
P steam = 0.1 MPa
P steam = 0.05 MPa
P steam = 0.01 MPa
Condensate pH
7
6
5
4
3
2
1
0
-1
100°
200°
300°
T (°C)

Fig. 3

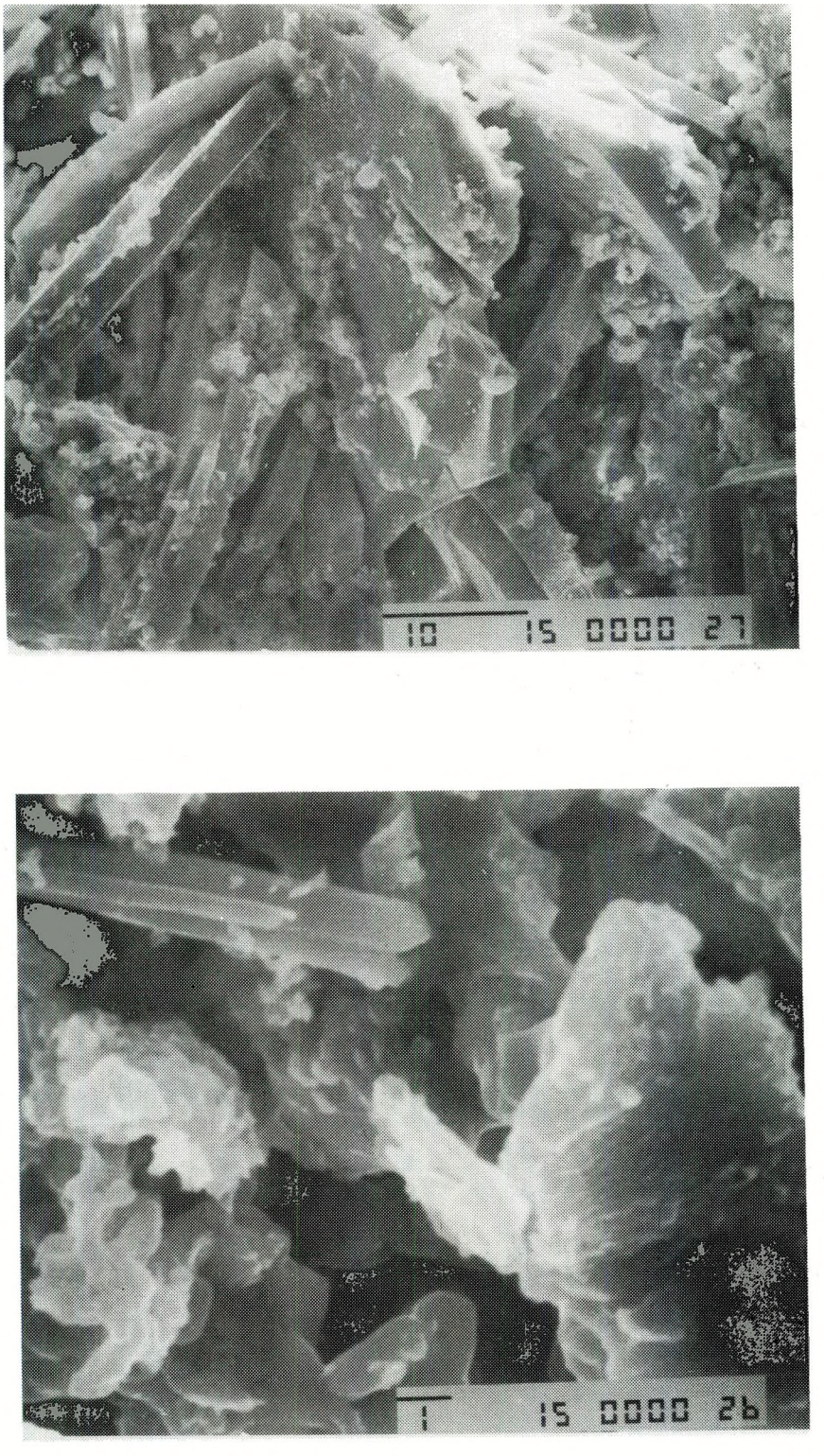

Fig. 4

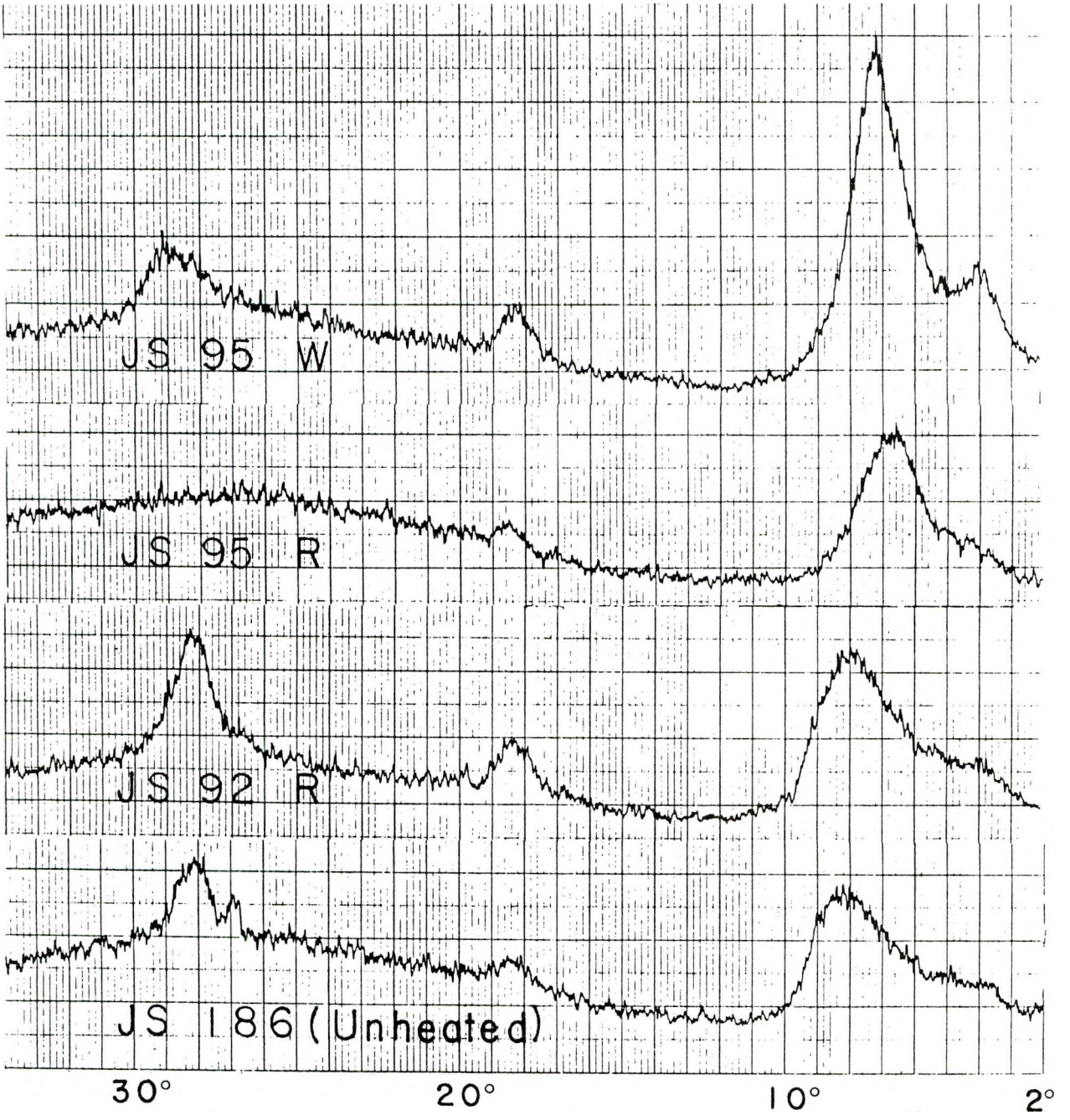

2θ Cu Kα

Fig. 5

Fig. 6A – JS186

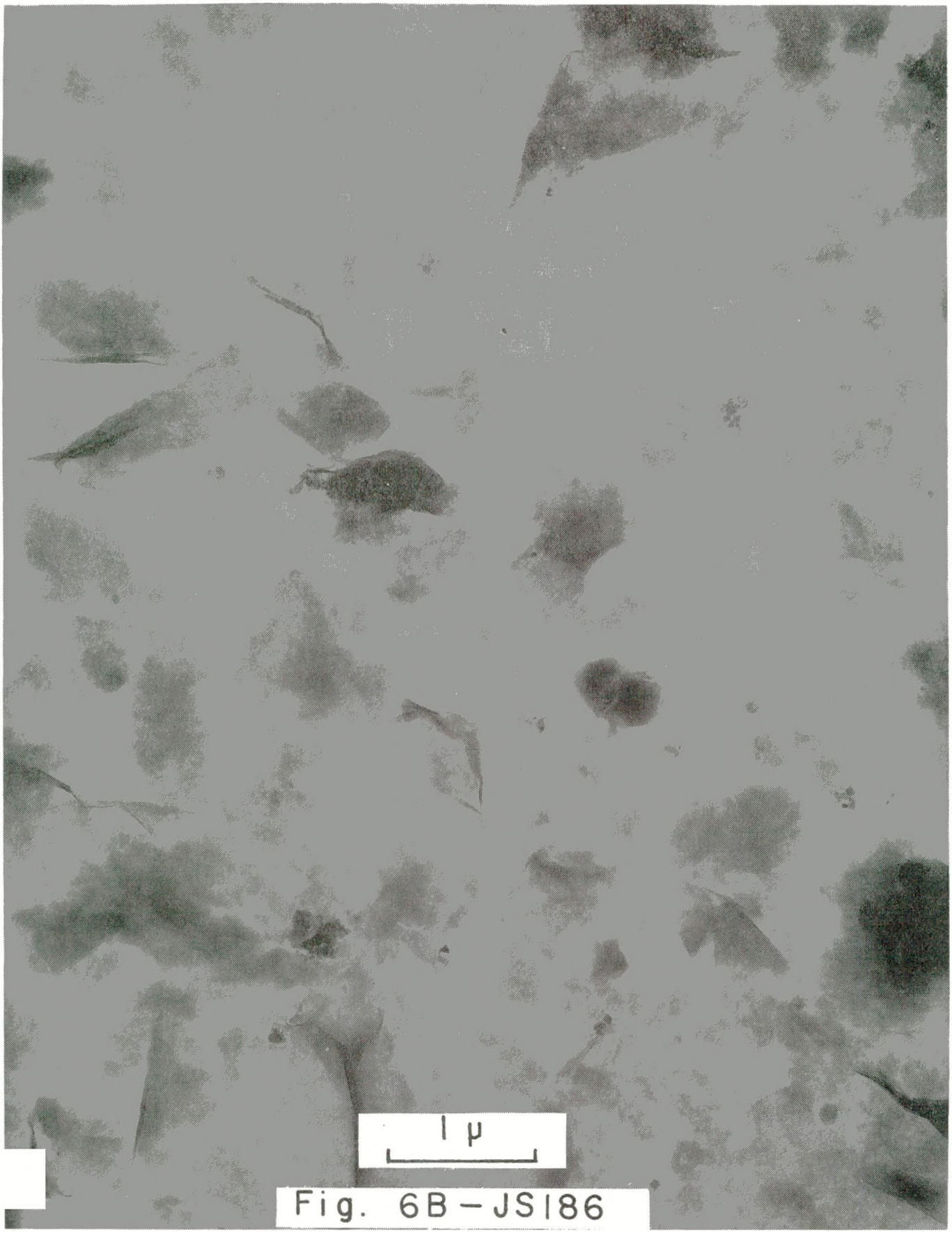

Fig. 6B – JS186

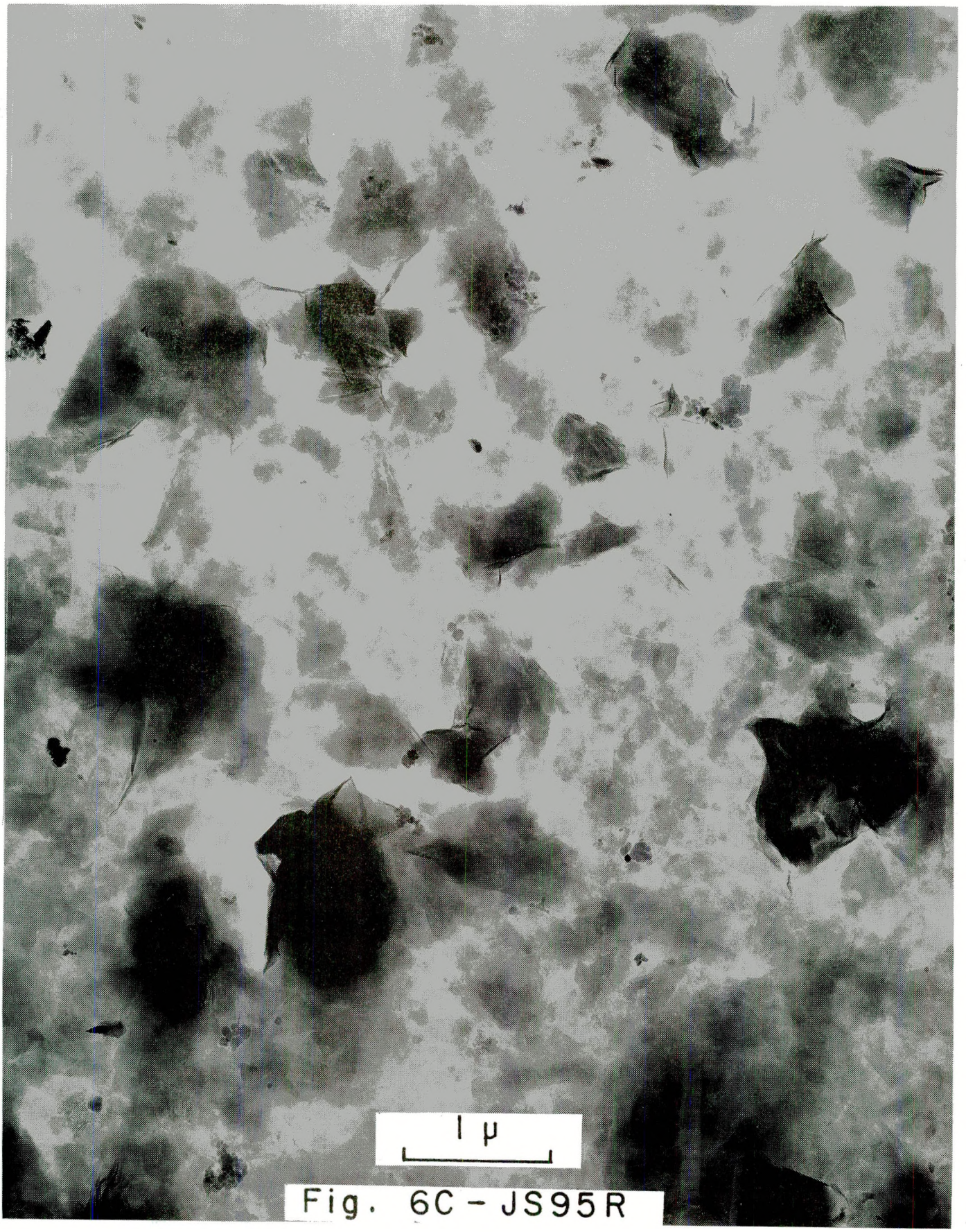

Fig. 6C - JS95R

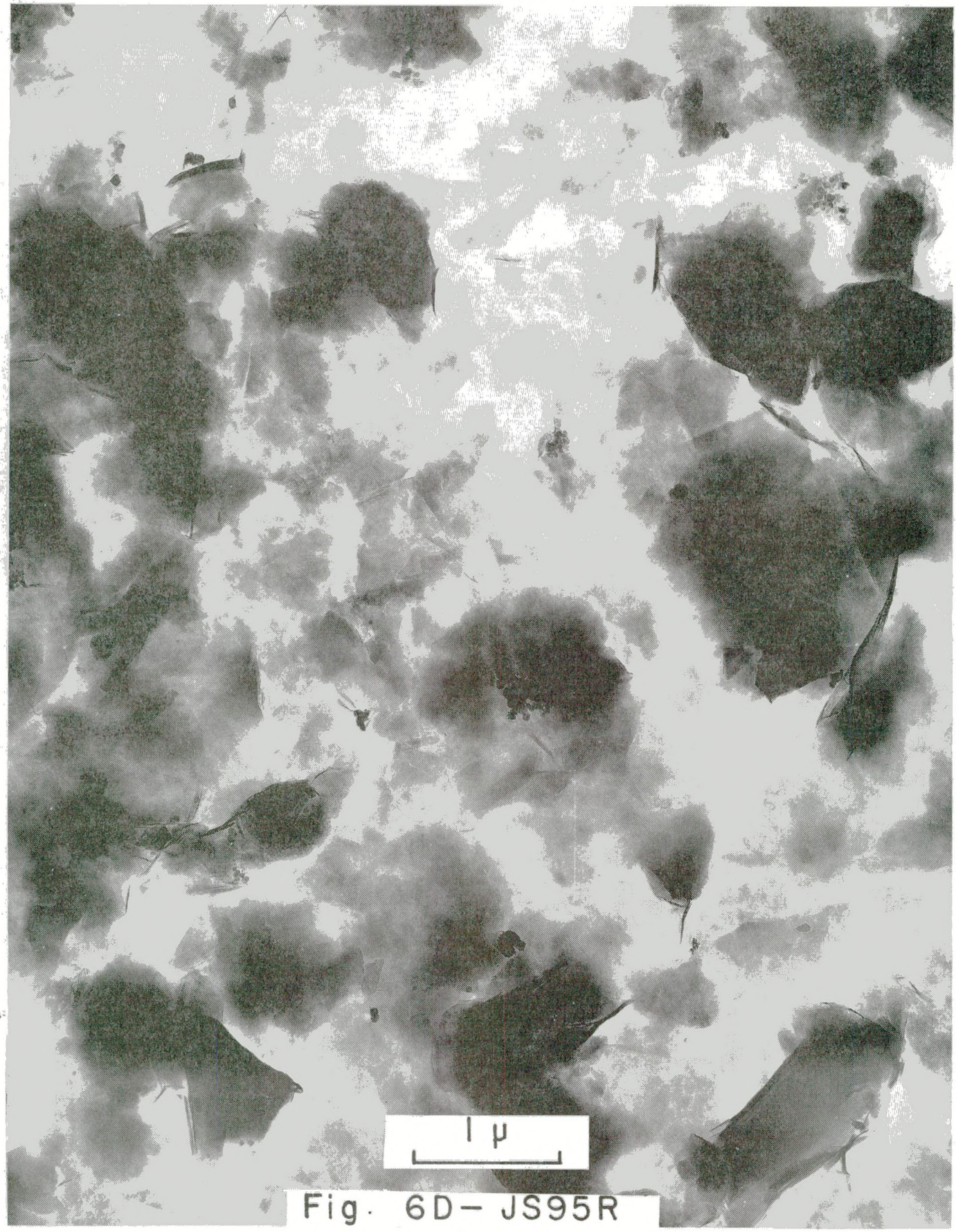

Fig. 6D – JS95R

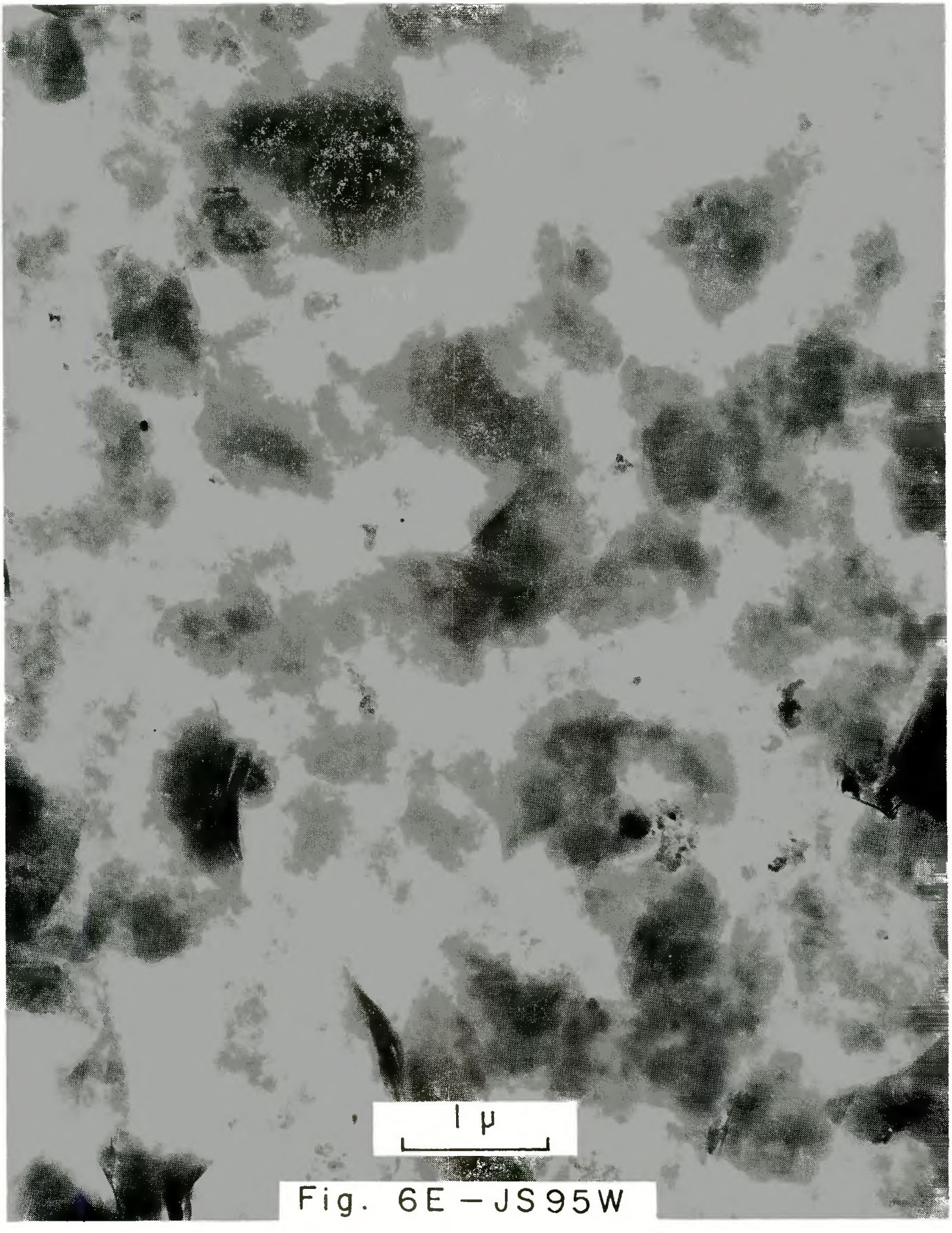

Fig. 6E – JS95W

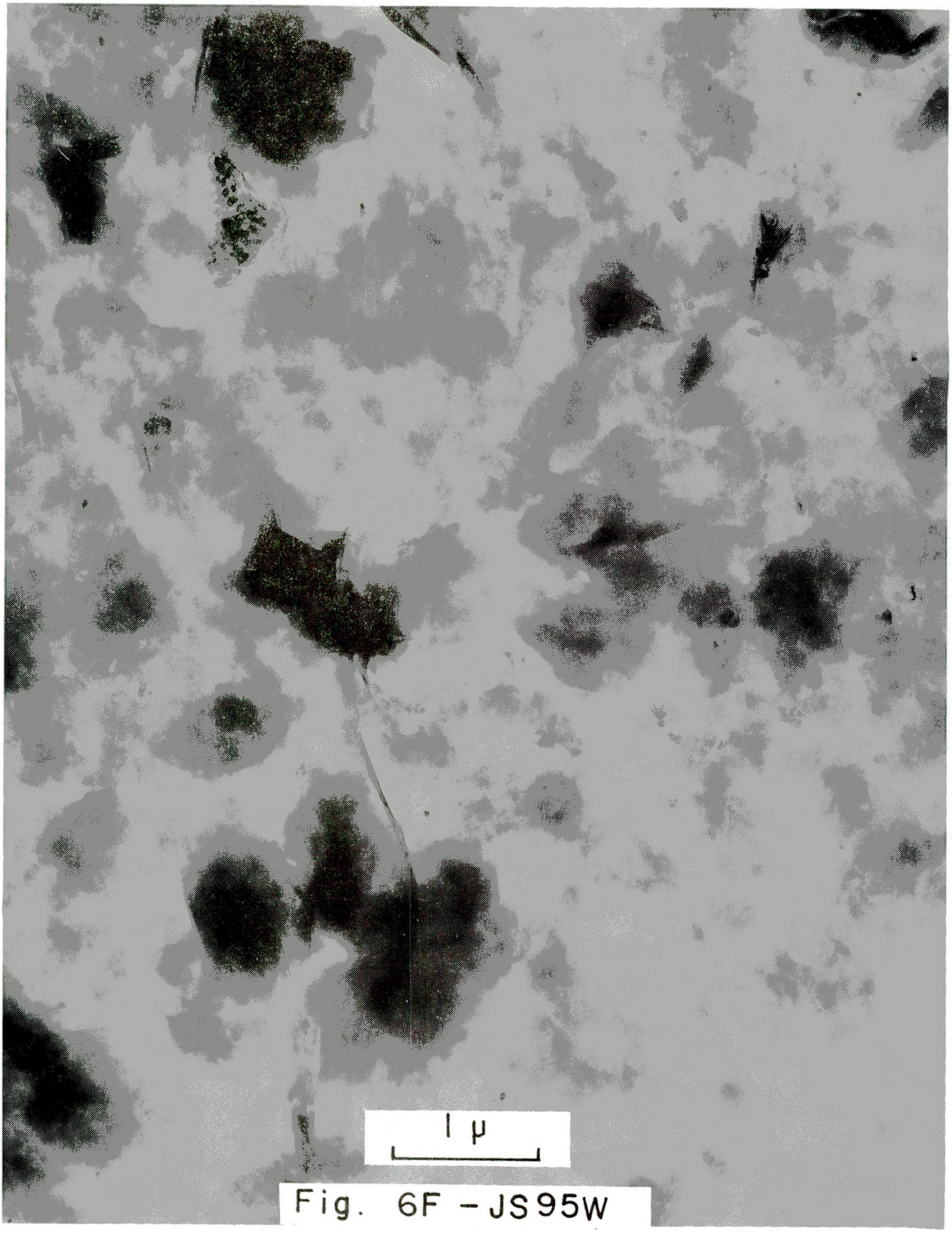

Fig. 6F - JS95W

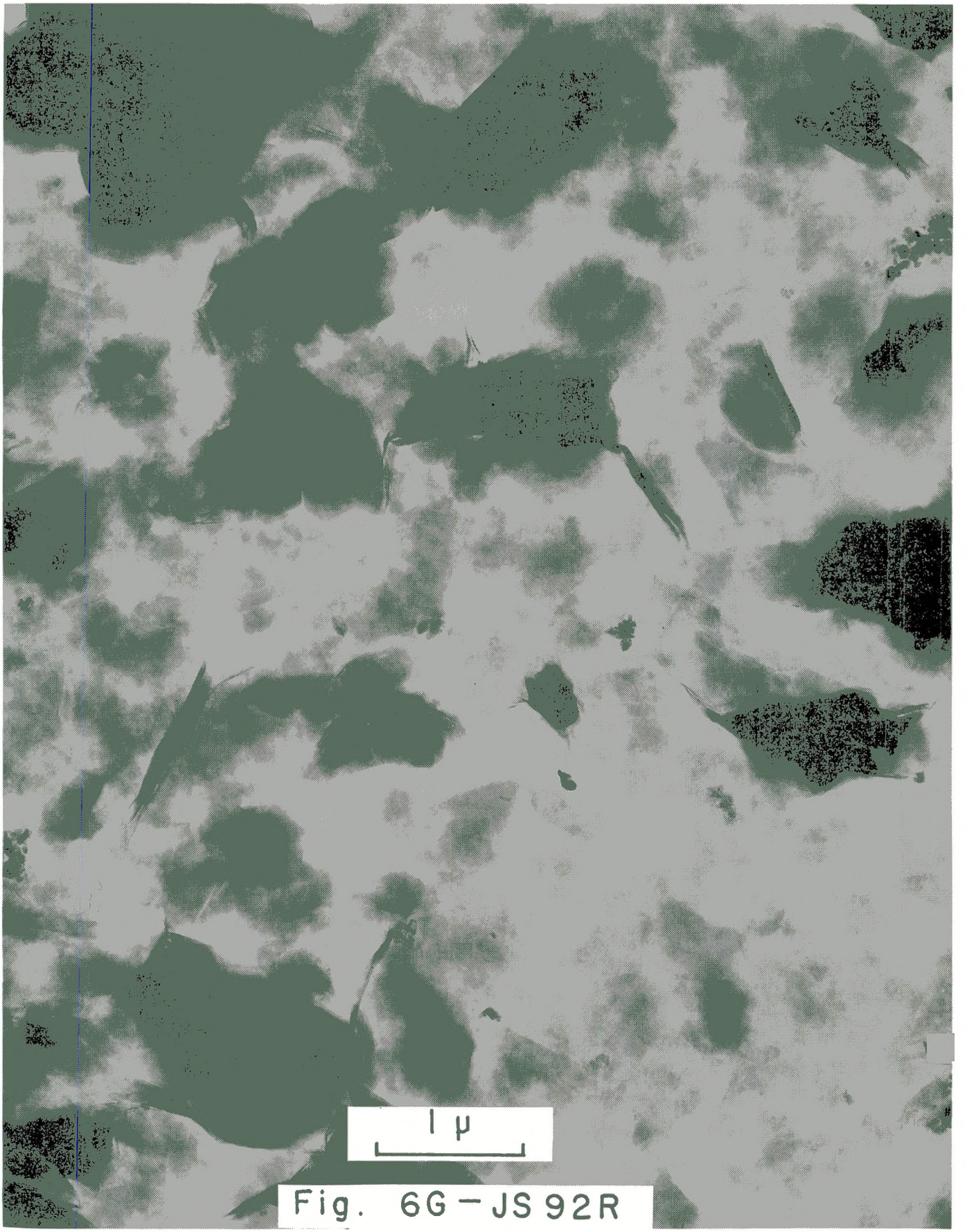

Fig. 6G – JS 92R

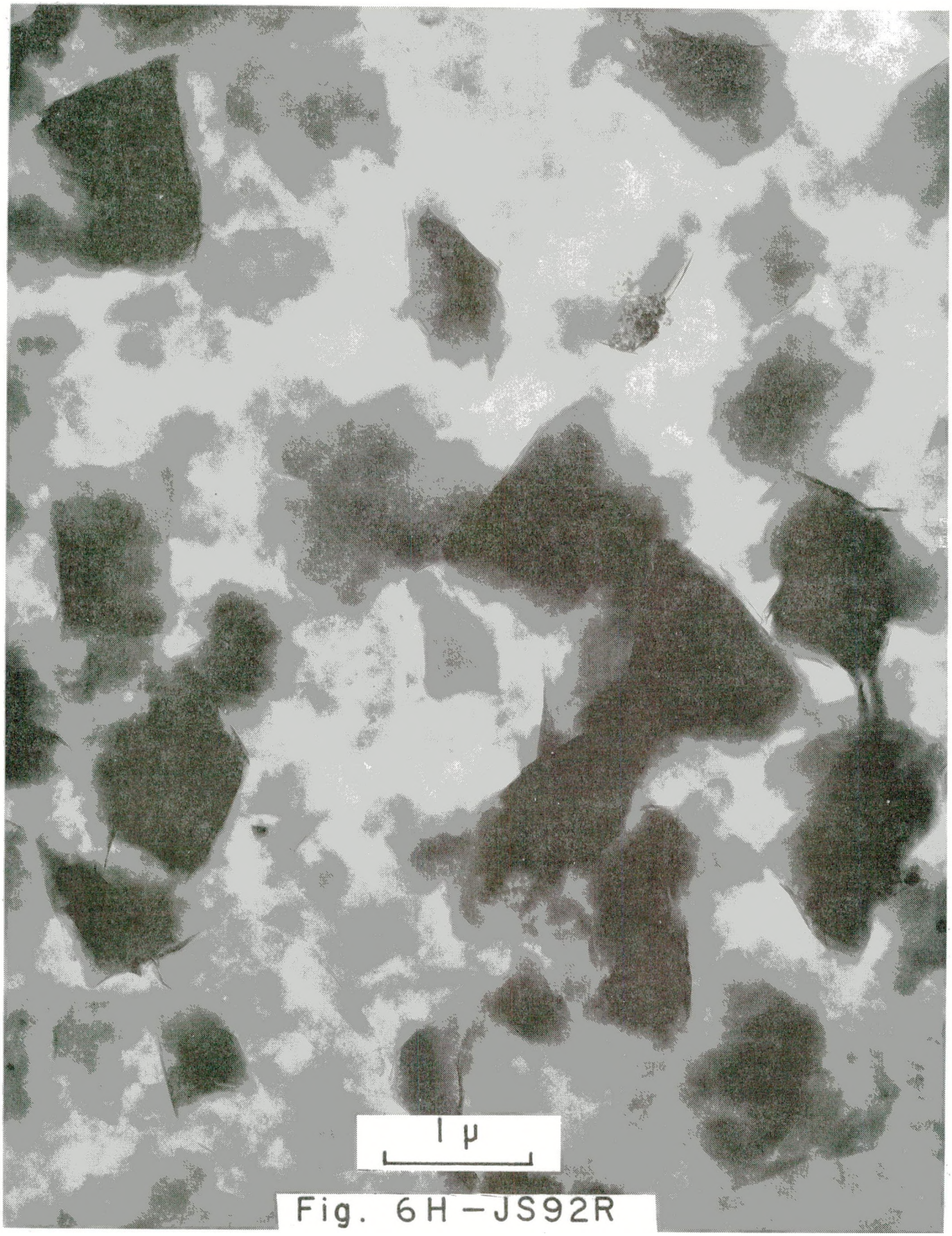

Fig. 6H-JS92R

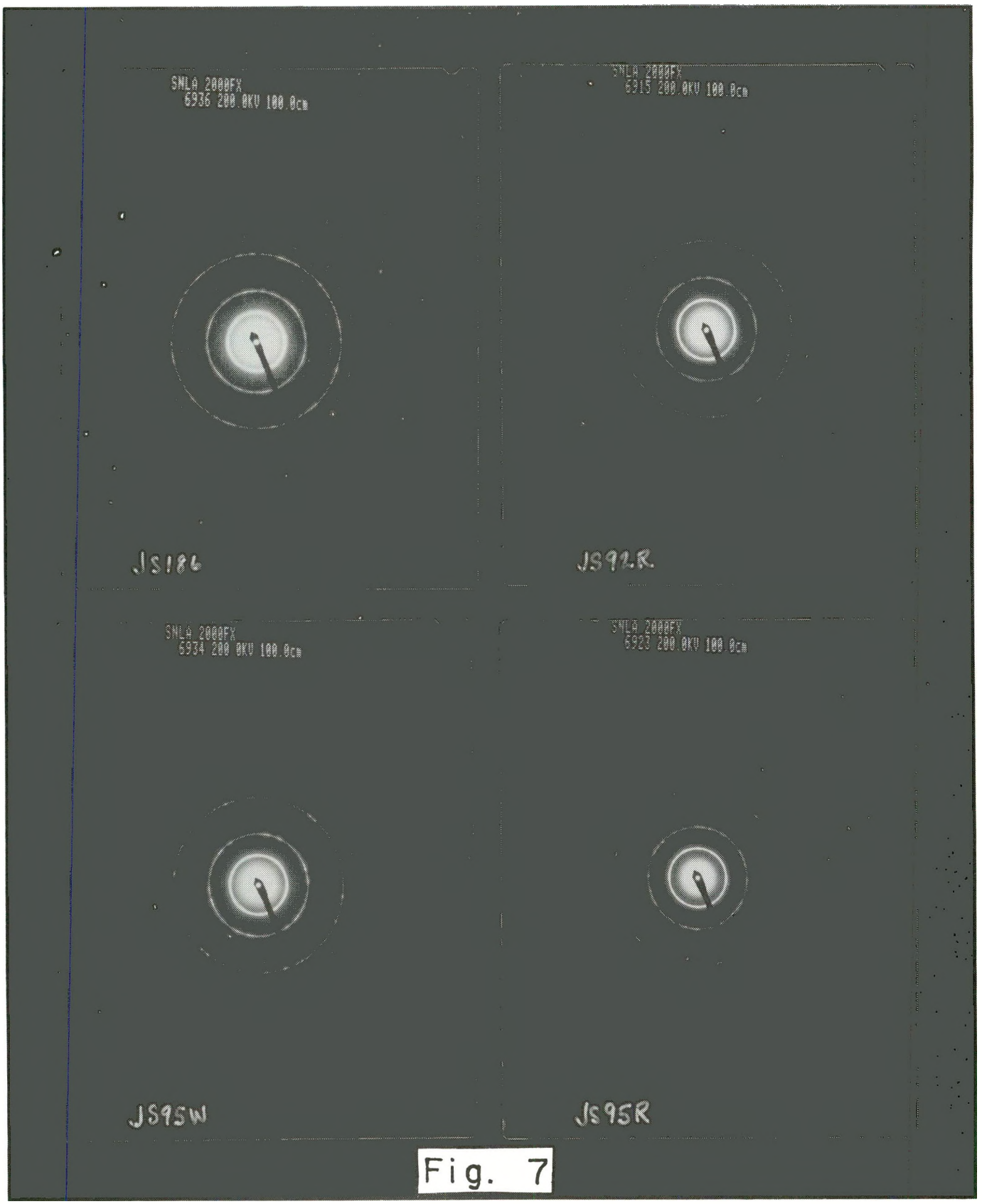
SMLA 2000FX
6936 200.0KV 100.0cm
JS18L
SMLA 2000FX
6915 200.0KV 100.0cm
JS91R
SMLA 2000FX
6934 200.0KV 100.0cm
JS95W
SMLA 2000FX
6923 200.0KV 100.0cm
JS95R

Fig. 7

This Page Intentionally Left Blank

Appendix A

Because the weep salts had strongly adhered to the inner surface of the hole wall as well as the heater surface, the raw weights of the samples collected contained contributions from chips of wall rock halite as well as scale from the corroded heater. The magnitude of each contribution was assessed by performing a chemical analysis on a split from each chip sample. The moisture content of a sample was obtained by drying a split of each sample at 133°C and determining the weight loss. The amount of insoluble residue was then obtained by washing each split free of soluble salts and weighing the dried residue. Contamination from the halite wall rock was estimated by an analysis of the leach fluid. The raw data generated in this manner is summarized in Table A-1, below.

In reducing the data it was assumed that this soluble fraction consisted of a simple mixture of two components; pure NaCl from the wall rock, and the mixture of salts that would be obtained if the average weep (Krumhansl, et al, 1990) were evaporated to dryness (Table A-2, column 2). It was also assumed that the brines did not change composition until they reached the face of the hole and dried.

Table A-1
Weight Percent of Salts Used in Computation

Element	Wall Rock	Average Weep Salt
Ca	0	0.16
Mg	0	6.71
K	0	5.45
Na	39.34	24.3
Cl	60.66	58.2
Br	0	0.58
SO4	0	4.60

Two properties of the weep fluids were particularly important in reducing the compositional data from the leach fluids (Fig. 1A); that Na/(K+Mg) = 2.1, s.d. = ±0.1, and that K/Mg = 0.8, s.d. = ±0.1. In the simplest case it was also assumed that all the salts from such a fluid were deposited. Thus, if the leach fluid analysis for a particular sample had a Na/(K+Mg) ratio of 26.94, the question first asked was how much sodium would have to be mixed with 100 grams of evaporated weep salt (Column 3, Table 2A) to form this mixture. Letting X be this quantity we can write (using the analyses from Column 2 Table 2):

$$\frac{24.3 + X}{(5.45 + 6.71)} = 26.94. \qquad (2)$$

With a little algebraic manipulation it follows that 303 grams of sodium, and thus 770.9 grams of sodium chloride, would have to be mixed with the 100 grams of dried weep salt to arrive at the experimentally measured ratio for this sample. Thus the chip sample was only 13% weep salt. If further, the

total weight of chips from this sample was 1470.9 grams, and the total dissolved salt load in 1 kg of brine is 290.8 grams, it follows that the grams of water that evaporated to give the weep salts, Y, can be given from the following equation.

$$Y = 0.1297 \times 1470.9 \times (1000 - 290.8)/290.8 = 465.3 \text{ g of water.} \quad (3)$$

In addition to computing the water coming from each segment sampled, two further corrections were applied to arrive at the total water influx. These were required because only 84% of the overcore was recovered and only 15.9% of the heater surface was scraped clean of salts. Thus, each evaluation of the brine influx was revised upward in proportion to the amount of unsampled surface area.

A second method of calculation involved an additional correction to take into account the fact that in a number of the samples analyzed the K/Mg ratio in the leach fluid was significantly larger than the value of a typical weep fluid, i.e. 0.8. It is known that, although a fluid such as brine A will boil essentially to dryness at 130°C., there may remain a small amount of magnesium chloride melt. It is suggested that this may have been pulled back from the interface by capillary action, and hence is missing from the chemical analysis. The second method of estimating brine influx involves computationally adding enough magnesium to the leach fluid analysis so that the K/Mg ratio is, in fact, lowered to 0.8. This theoretically altered bulk fluid composition is then used to compute a new Na/(K+Mg) ratio. After that the computational procedure is the same as outlined above. The net effect of this procedure was to increase the weight of the weep salts which, in theory, were associated with the rock salt chips in any given sample. Hence, fluid influx predictions using this methodology are slightly larger than with the first method outlined.

Table A-2
Analytic Results For Chip Samples

Fig. 1 - Sample 1

% Na	37.3	% Cl	59.6
% K	.91	% Br	N.D.
% Mg	.54	% SO_4	1.29
% Ca	.33		

Fig. 1 - Sample 2

% Na	32.6	% Cl	57.9
% K	3.4	% Br	N.D.
% Mg	2.4	% SO_4	3.6
% Ca	0.08		

Fig. 1 - Sample 3

% Na	35.3	% Cl	59.3
% K	1.7	% Br	N.D.
% Mg	1.6	% SO_4	1.9
% Ca	0.08		

Fig. 1 - Sample 4

% Na	35.2	% Cl	59.7
% K	1.6	% Br	N.D.
% Mg	1.7	% SO_4	1.6
% Ca	0.08		

Fig. 1 - Sample 5

% Na	35.3	% Cl	59.5
% K	2.1	% Br	N.D.
% Mg	1.4	% SO_4	1.6
% Ca	0.05		

Fig. 1 - Sample 6

% Na	33.1	% Cl	58.3
% K	3.6	% Br	N.D.
% Mg	2.1	% SO_4	2.90
% Ca	0.05		

Fig. 1 - Sample 7

% Na	33.2	% Cl	58.1
% K	3.8	% Br	N.D.
% Mg	1.9	% SO_4	2.9
% Ca	0.07		

Fig. 1 - Sample 8

% Na	34.4	% Cl	58.4
% K	2.6	% Br	N.D.
% Mg	1.7	% SO_4	2.8
% Ca	0.07		

Fig. 1 - Sample 9A

% Na	36.3	% Cl	59.3
% K	1.7	% Br	N.D.
% Mg	0.96	% SO_4	1.6
% Ca	0.12		

Fig. 1 - Sample 9B

% Na	37.2	% Cl	59.8
% K	1.0	% Br	N.D.
% Mg	0.72	% SO_4	1.1
% Ca	0.14		

Fig. 1 - Sample 10

% Na	34.6	% Cl	59.1
% K	2.0	% Br	N.D.
% Mg	1.9	% SO_4	2.2
% Ca	0.11		

Fig. 1 - Sample 11

% Na	35.4	% Cl	59.1
% K	1.7	% Br	N.D.
% Mg	1.5	% SO_4	2.3
% Ca	0.09		

Fig. 1 - Sample 12

% Na	32.3	% Cl	59.7
% K	2.4	% Br	N.D.
% Mg	3.1	% SO_4	2.3
% Ca	0.17		

Fig. 1 - Sample 13

% Na	28.8	% Cl	58.3
% K	4.1	% Br	0.31
% Mg	4.5	% SO_4	3.9
% Ca	0.09		

Fig. 1 - Sample 14

% Na	35.6	% Cl	58.7
% K	1.6	% Br	0.09
% Mg	1.4	% SO_4	2.6
% Ca	0.09		

Fig. 1 - Sample 15

% Na	37.5	% Cl	59.8
% K	0.76	% Br	N.D.
% Mg	0.73	% SO_4	1.2
% Ca	0.06		

Fig. 1 - Sample 16

% Na	36.9	% Cl	59.8
% K	0.95	% Br	0.08
% Mg	1.0	% SO_4	1.2
% Ca	0.07		

Fig. 1 - Sample 17

% Na	36.4	% Cl	59.9
% K	1.1	% Br	0.10
% Mg	1.2	% SO_4	1.2
% Ca	0.06		

Fig. 1 - Sample 18

% Na	34.4	% Cl	59.2
% K	2.3	% Br	0.13
% Mg	1.9	% SO_4	2.0
% Ca	0.05		

Fig. 1 - Sample 19

% Na	36.1	% Cl	58.9
% K	1.4	% Br	0.08
% Mg	1.2	% SO_4	2.2
% Ca	0.07		

Fig. 1 - Sample 20

% Na	36.1	% Cl	60.4
% K	1.5	% Br	0.08
% Mg	1.3	% SO_4	0.61
% Ca	0.05		

Fig. 1 - Sample 21

% Na	38.3	% Cl	60.1
% K	0.22	% Br	N.D.
% Mg	0.36	% SO_4	0.78
% Ca	0.25		

Fig. 1 - Sample 22

% Na	27.9	% Cl	60.0
% K	3.6	% Br	0.39
% Mg	5.3	% SO_4	2.6
% Ca	0.13		

Fig. 1 - Sample 23

% Na	23.8	% Cl	57.1
% K	6.5	% Br	0.46
% Mg	6.5	% SO_4	5.7
% Ca	0.05		

Fig. 1 - Sample 24

% Na	30.8	% Cl	57.0
% K	3.8	% Br	0.20
% Mg	3.3	% SO_4	4.8
% Ca	0.05		

Fig. 1 - Sample 25

% Na	38.0	% Cl	59.6
% K	0.59	% Br	N.D.
% Mg	0.43	% SO_4	1.3
% Ca	0.07		

Fig. 1 - Sample 26

% Na	38.5	% Cl	60.1
% K	0.42	% Br	N.D.
% Mg	0.28	% SO_4	0.74
% Ca	0.02		

Fig. 1 - Sample 27

% Na	38.1	% Cl	60.5
% K	0.36	% Br	N.D.
% Mg	0.29	% SO_4	0.69
% Ca	0.05		

Fig. 1 - Sample 28

% Na	38.1	% Cl	60.0
% K	0.43	% Br	N.D.
% Mg	0.46	% SO_4	0.92
% Ca	0.10		

Fig. 1 - Sample 29

% Na	39.1	% Cl	60.2
% K	0.25	% Br	N.D.
% Mg	0.48	% SO_4	0.80
% Ca	0.21		

Fig. 1 - Sample 30

% Na	35.3	% Cl	56.2
% K	1.6	% Br	N.D.
% Mg	1.3	% SO_4	5.4
% Ca	0.24		

Fig. 1 - Sample 31

% Na	28.6	% Cl	56.3
% K	4.5	% Br	0.37
% Mg	4.2	% SO_4	5.8
% Ca	0.09		

Fig. 1 - Sample 32

% Na	30.7	% Cl	57.6
% K	5.1	% Br	N.D.
% Mg	2.8	% SO_4	3.7
% Ca	0.06		

Heater, 0 - 1 foot down from the top, Sample 33

% Na	36.5	% Cl	59.8
% K	0.85	% Br	N.D.
% Mg	1.1	% SO_4	1.4
% Ca	0.36		

Heater, 1 - 2 feet down from the top, Sample 34

% Na	34.5	% Cl	58.5
% K	2.0	% Br	0.41
% Mg	1.9	% SO_4	2.7
% Ca	0.12		

Heater, 2 - 3 feet down from the top, Sample 35

% Na	27.4	% Cl	55.0
% K	5.7	% Br	0.48
% Mg	4.3	% SO_4	6.9
% Ca	0.07		

Heater, 3 - 4 feet down from the top, Sample 36

% Na	27.2	% Cl	55.2
% K	6.7	% Br	0.45
% Mg	4.1	% SO_4	6.3
% Ca	0.07		

Heater, 4 - 5 feet down from the top, Sample 37

% Na	17.2	% Cl	52.5
% K	16.0	% Br	0.55
% Mg	6.0	% SO_4	7.8
% Ca	0.04		

Heater, 5 - 6 feet down from the top, Sample 38

% Na	24.2	% Cl	55.3
% K	19.3	% Br	0.75
% Mg	0.22	% SO_4	0.02
% Ca	0.10		

Heater, 6 - 7 feet down from the top, Sample 39

% Na	18.3	% Cl	60.8
% K	6.0	% Br	0.91
% Mg	10.3	% SO_4	3.6
% Ca	0.07		

Heater, 7 - 8 feet down from the top, Sample 40

% Na	26.1	% Cl	58.3
% K	5.0	% Br	0.62
% Mg	5.7	% SO_4	4.1
% Ca	0.008		

Heater, 8 - 8.33 feet down from the top, Sample 41

% Na	33.7	% Cl	58.8
% K	2.6	% Br	N.D.
% Mg	1.9	% SO_4	2.6
% Ca	0.33		

Fig. 1A

WEEPS

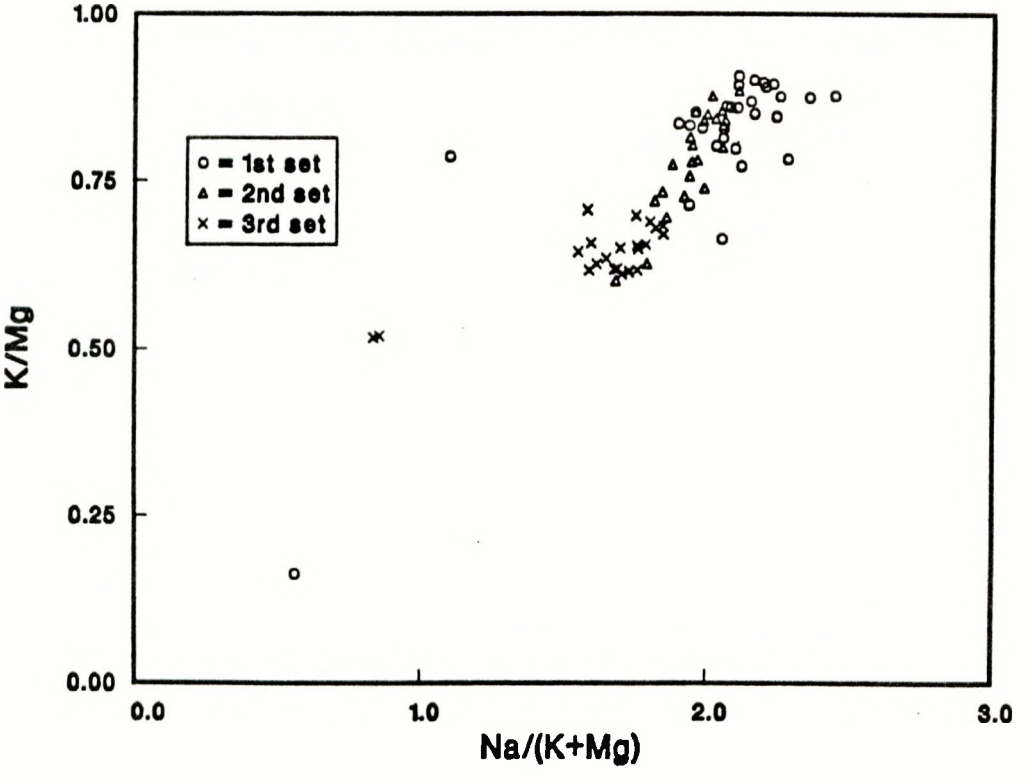

DISTRIBUTION

UC-721 (531)

FEDERAL AGENCIES

U. S. Department of Energy, (5)
Office of Civilian Radioactive Waste Management
Attn: Deputy Director, RW-2
Associate Director, RW-10
Office of Program Administration and Resources Management
Associate Director, RW-20
Office of Facilities Siting and Development
Associate Director, RW-30
Office of Systems Integration and Regulations
Associate Director, RW-40
Office of External Relations and Policy
Forrestal Building
Washington, DC 20585

U. S. Department of Energy (3)
Albuquerque Operations Office
Attn: J. E. Bickel
R. Marquez, Director
Public Affairs Division
P.O. Box 5400
Albuquerque, NM 87185

U. S. Department of Energy
Attn: National Atomic Museum Library
Albuquerque Operations Office
P. O. Box 5400
Albuquerque, NM 87185

U. S. Department of Energy (4)
WIPP Project Office (Carlsbad)
Attn: Vernon Daub
J. A. Mewhinney
P.O. Box 3090
Carlsbad, NM 88221

U. S. Department of Energy
Research & Waste Management Division
Attn: Director
P. O. Box E
Oak Ridge, TN 37831

U.S. Department of Energy
Richland Operations Office
Nuclear Fuel Cycle & Production Division
Attn: R. E. Gerton
P.O. Box 500
Richland, WA 99352

U. S. Department of Energy (1)
Attn: Edward Young
Room E-178
GAO/RCED/GTN
Washington, DC 20545

U. S. Department of Energy (6)
Office of Environmental Restoration and Waste Management
Attn: Jill Lytle, EM30
Mark Frei, EM-34 (3)
Mark Duff, EM-34
Clyde Frank, EM-50
Washington, DC 20585

U. S. Department of Energy (3)
Office of Environment, Safety and Health
Attn: Ray Pelletier, EH-231
Kathleen Taimi, EH-232
Carol Borgstrom, EH-25
Washington, DC 20585

U. S. Department of Energy (2)
Idaho Operations Office
Fuel Processing and Waste Management Division
785 DOE Place
Idaho Falls, ID 83402

U.S. Department of Energy
Savannah River Operations Office
Defense Waste Processing Facility Project Office
Attn: W. D. Pearson
P.O. Box A
Aiken, SC 29802

U.S. Environmental Protection Agency (2)
Attn: Ray Clark
Office of Radiation Programs (ANR-460)
Washington, DC 20460

U.S. Geological Survey
Branch of Regional Geology
Attn: R. Snyder
MS913, Box 25046
Denver Federal Center
Denver, CO 80225

U.S. Geological Survey
Conservation Division
Attn: W. Melton
P.O. Box 1857
Roswell, NM 88201

U.S. Geological Survey (2)
Water Resources Division
Attn: Kathy Peter
Suite 200
4501 Indian School, NE
Albuquerque, NM 87110

U.S. Nuclear Regulatory Commission (4)
Attn: Joseph Bunting, HLEN 4H3 OWFN
Ron Ballard, HLGP 4H3 OWFN
Jacob Philip
NRC Library
Mail Stop 623SS
Washington, DC 20555

Boards

Defense Nuclear Facilities Safety Board
Attn: Dermot Winters
Suite 700
625 Indiana Ave., NW
Washington, DC 20004

U. S. Department of Energy
Advisory Committee on Nuclear Facility Safety
Attn: Merritt E. Langston, AC21
Washington, DC 20585

Nuclear Waste Technical Review Board (2)
Attn: Dr. Don A. Deere
Dr. Sidney J. S. Parry
Suite 910
1100 Wilson Blvd.
Arlington, VA 22209-2297

Richard Major
Advisory Committee on Nuclear Waste
Nuclear Regulatory Commission
7920 Norfolk Avenue
Bethesda, MD 20814

STATE AGENCIES

Environmental Evaluation Group (3)
Attn: Library
Suite F-2
7007 Wyoming Blvd., N.E.
Albuquerque, NM 87109

New Mexico Bureau of Mines and Mineral Resources (2)
Attn: F. E. Kottolowski, Director
J. Hawley
Socorro, NM 87801

NM Department of Energy & Minerals
Attn: Librarian
2040 S. Pacheco
Santa Fe, NM 87505

NM Environmental Improvement Division
Attn: Deputy Director
1190 St. Francis Drive
Santa Fe, NM 87503

LABORATORIES/CORPORATIONS

Battelle Pacific Northwest Laboratories (6)
Attn: D. J. Bradley, K6-24
J. Relyea, H4-54
R. E. Westerman, P8-37
S. Bates, K2-57
H. C. Burkholder, P7-41
L. Pederson, K6-47
Battelle Boulevard
Richland, WA 99352

Savannah River Laboratory (6)
Attn: N. Bibler
E. L. Albenisius
M. J. Plodinec
G. G. Wicks
C. Jantzen
J. A. Stone
Aiken, SC 29801

George Dymmel
SAIC
101 Convention Center Dr.
Las Vegas, NV 89109

INTERA Technologies, Inc. (4)
Attn: G. E. Grisak
J. F. Pickens
A. Haug
A. M. LeVenue
Suite #300
6850 Austin Center Blvd.
Austin, TX 78731

INTERA Technologies, Inc.
Attn: Wayne Stensrud
P.O. Box 2123
Carlsbad, NM 88221

IT Corporation (2)
Attn: R. F. McKinney
J. Myers
Regional Office - Suite 700
5301 Central Avenue, NE
Albuquerque, NM 87108

IT Corporation (2)
Attn: D. E. Deal
P.O. Box 2078
Carlsbad, NM 88221

Charles R. Hadlock
Arthur D. Little, Inc.
Acorn Park
Cambridge, MA 02140-2390

Los Alamos Scientific Laboratory
Attn: B. Erdal, CNC-11
Los Alamos, NM 87545

Oak Ridge National Laboratory (4)
Attn: T. F. Lomenick
Box 2009
Oak Ridge, TN 37831

RE/SPEC, Inc.
Attn: W. Coons
P. F. Gnirk
4775 Indian School Rd. NE
Suite 300
Albuquerque NM 87110

RE/SPEC, Inc. (7)
Attn: L. L. Van Sambeek
G. Callahan
T. Pfeifle
J. L. Ratigan
P. O. Box 725
Rapid City, SD 57709

Center for Nuclear Waste
Regulatory Analysis (4)
Attn: P. K. Nair
Southwest Research Institute
6220 Culebra Road
San Antonio, TX 78228-0510

Science Applications
International Corporation
Attn: Howard R. Pratt,
Senior Vice President
10260 Campus Point Drive
San Diego, CA 92121

Science Applications
International Corporation
Attn: Michael B. Gross
Ass't. Vice President
Suite 1250
160 Spear Street
San Francisco, CA 94105

Systems, Science, and Software (2)
Attn: E. Peterson
Box 1620
La Jolla, CA 92038

Westinghouse Electric Corporation (7)
Attn: Library
Lamar Trego
W. P. Poirer
W. R. Chiquelin
V. F.Likar
D. J. Moak
R. F. Kehrman
P. O. Box 2078
Carlsbad, NM 88221

Weston Corporation (1)
Attn: David Lechel
Suite 1000
5301 Central Avenue, NE
Albuquerque, NM 87108

UNIVERSITIES

University of Arizona
Attn: J. G. McCray
Department of Nuclear Engineering
Tucson, AZ 85721

University of New Mexico (2)
Geology Department
Attn: D. G. Brookins
Library
Albuquerque, NM 87131

Pennsylvania State University
Materials Research Laboratory
Attn: Della Roy
University Park, PA 16802

Texas A&M University
Center of Tectonophysics
College Station, TX 77840

G. Ross Heath
College of Ocean
and Fishery Sciences
University of Washington
Seattle, WA 98195

INDIVIDUALS

Dennis W. Powers
Star Route Box 87
Anthony, TX 79821

LIBRARIES

Thomas Brannigan Library
Attn: Don Dresp, Head Librarian
106 W. Hadley St.
Las Cruces, NM 88001

Hobbs Public Library
Attn: Ms. Marcia Lewis, Librarian
509 N. Ship Street
Hobbs, NM 88248

New Mexico State Library
Attn: Ms. Ingrid Vollenhofer
P.O. Box 1629
Santa Fe, NM 87503

New Mexico Tech
Martin Speere Memorial Library
Campus Street
Socorro, NM 87810

Pannell Library
Attn: Ms. Ruth Hill
New Mexico Junior College
Lovington Highway
Hobbs, NM 88240

WIPP Public Reading Room
Attn: Director
Carlsbad Public Library
101 S. Halagueno St.
Carlsbad, NM 88220

Government Publications Department
General Library
University of New Mexico
Albuquerque, NM 87131

THE SECRETARY'S BLUE RIBBON PANEL ON WIPP

Dr. Thomas Bahr
New Mexico Water Resources Institute
New Mexico State University
Box 3167
Las Cruces, NM 88003-3167

Mr. Leonard Slosky
Slosky and Associates
Suite 1400
Bank Western Tower
1675 Tower
Denver, Colorado 80202

Mr. Newal Squyres
Eberle and Berlin
P. O. Box 1368
Boise, Idaho 83701

Dr. Arthur Kubo
Vice President
BDM International, Inc.
7915 Jones Branch Drive
McLean, VA 22102

Mr. Robert Bishop
Nuclear Management Resources Council
Suite 300
1776 I Street, NW
Washington, DC 20006-2496

NATIONAL ACADEMY OF SCIENCES, WIPP PANEL

Dr. Charles Fairhurst, Chairman
Department of Civil and Mineral Engineering
University of Minnesota
500 Pillsbury Dr. SE
Minneapolis, MN 55455

Dr. John O. Blomeke
Route 3
Sandy Shore Drive
Lenoir City, TN 37771

Dr. John D. Bredehoeft
Western Region Hydrologist
Water Resources Division
U.S. Geological Survey (M/S 439)
345 Middlefield Road
Menlo Park, CA 94025

Dr. Karl P. Cohen
928 N. California Avenue
Palo Alto, CA 94303

Dr. Fred M. Ernsberger
250 Old Mill Road
Pittsburgh, PA 15238

Dr. Rodney C. Ewing
Department of Geology
University of New Mexico
200 Yale, NE
Albuquerque, NM 87131

B. John Garrick
Pickard, Lowe & Garrick, Inc.
2260 University Drive
Newport Beach, CA 92660

John W. Healy
51 Grand Canyon Drive
Los Alamos, NM 87544

Leonard F. Konikow
U.S. Geological Survey
431 National Center
Reston, VA 22092

Jeremiah O'Driscoll
505 Valley Hill Drive
Atlanta, GA 30350

Dr. D'Arcy A. Shock
233 Virginia
Ponca City, OK 74601

Dr. Christopher G. Whipple
Electric Power Research Institute
3412 Hillview Avenue
Palo Alto, CA 94303

Dr. Peter B. Myers, Staff Director
National Academy of Sciences
Committee on Radioactive Waste Management
2101 Constitution Avenue
Washington, DC 20418

Dr. Geraldine Grube
Board on Radioactive Waste Management
GF462
2101 Constitution Avenue
Washington, DC 20418

Dr. Ina Alterman
Board on Radioactive Waste Management
GF462
2101 Constitution Avenue
Washington, DC 20418

FOREIGN ADDRESSES

Studiecentrum Voor Kernenergie
Centre D'Energie Nucleaire
Attn: Mr. A. Bonne
SCK/CEN
Boeretang 200
B-2400 Mol
BELGIUM

Atomic Energy of Canada, Ltd. (2)
Whiteshell Research Estab.
Attn: Peter Haywood
John Tait
Pinewa, Manitoba, CANADA
ROE 1LO

Dr. D. K. Mukerjee
Ontario Hydro Research Lab
800 Kipling Avenue
Toronto, Ontario, CANADA
M8Z 5S4

Mr. Francois Chenevier, Director (2)
ANDRA
Route du Panorama Robert Schumann
B.P.38
92266 Fontenay-aux-Roses Cedex
FRANCE

Mr. Jean-Pierre Olivier
OECD Nuclear Energy Agency
Division of Radiation Protection
and Waste Management
38, Boulevard Suchet
75016 Paris, FRANCE

Claude Sombret
Centre D'Etudes Nucleaires
De La Vallee Rhone
CEN/VALRHO
S.D.H.A. BP 171
30205 Bagnols-Sur-Ceze
FRANCE

Bundesministerium fur Forschung und
Technologie
Postfach 200 706
5300 Bonn 2
FEDERAL REPUBLIC OF GERMANY

Bundesanstalt fur Geowissenschaften
und Rohstoffe
Attn: Michael Langer
Postfach 510 153
3000 Hannover 51
FEDERAL REPUBLIC OF GERMANY

Hahn-Meitner-Institut fur
Kernforschung
Attn: Werner Lutze
Glienicker Strasse 100
100 Berlin 39
FEDERAL REPUBLIC OF GERMANY

Institut fur Tieflagerung (4)
Attn: K. Kuhn
Theodor-Heuss-Strasse 4
D-3300 Braunschweig
FEDERAL REPUPLIC OF GERMANY

Kernforschug Karlsruhe
Attn: K. D. Closs
Postfach 3640
7500 Karlsruhe
FEDERAL REPUBLIC OF GERMANY

Physikalisch-Technische Bundesanstalt
Attn: Peter Brenneke
Postfach 33 45
D-3300 Braunschweig
FEDERAL REPUBLIC OF GERMANY

D. R. Knowles
British Nuclear Fuels, plc
Risley, Warrington, Cheshire WA3 6AS
1002607 GREAT BRITAIN

Shingo Tashiro
Japan Atomic Energy Research
Institute
Tokai-Mura, Ibaraki-Ken
319-11 JAPAN

Netherlands Energy Research
Foundation ECN (2)
Attn: Tuen Deboer, Mgr.
L. H. Vons
3 Westerduinweg
P.O. Box 1
1755 ZG Petten, THE NETHERLANDS

Svensk Karnbransleforsorjning AB
Attn: Fred Karlsson
Project KBS
Karnbranslesakerhet
Box 5864
10248 Stockholm, SWEDEN

SANDIA INTERNAL

400 L. D. Tyler
1510 J. C. Cummings
1520 C. W. Peterson
1521 J. G. Arguello
1521 H. S. Morgan
3141 S. A. Landenberger (5)
3145 Document Processing (8) for DOE/OSTI
3151 G. C. Claycomb (3)
6230 R. K. Traeger
6232 W. R. Wawersik
6233 J. L. Krumhansl (3)
6300 T. O. Hunter
6310 T. E. Blejwas, Actg.
6313 L. E. Shephard
6340 W. D. Weart
6340 S. Y. Pickering
6341 R. C. Lincoln
6341 Staff (7)
6341 Sandia WIPP Central Files (10)
6342 D. R. Anderson
6342 Staff (11)
6343 T. M. Schultheis
6343 Staff (2)
6344 E. Gorham
6344 Staff (8)
6345 A. R. Lappin
6345 Staff (9)
6346 J. R. Tillerson
6346 Staff (7)
8523 R. C. Christman (SNLL Library)
9300 J. E. Powell
9310 J. D. Plimpton
9320 M. J. Navratil
9325 R. L. Rutter
9325 J. T. McIlmoyle
9330 J. D. Kennedy
9333 O. Burchett
9333 J. W. Mercer
9334 P. D. Seward

Org.	Bldg.	Name	Rec'd by	Org.	Bldg.	Name	Rec'd by